ISSN 1 746-7233, England, UK
World Journal of Modelling and Simulation
Vol. 13 (2017) No. 1, pp. 3-11

Carotid artery stenosis pre-assessment by relationship derived from two-dimensional patient-specific model and throat velocity ratio*

Arpapan Prakobkarn[1], Natee Ina[2], Sakchai Saeheng[3], Surapong Chatpun[1 †]

[1] Institute of Biomedical Engineering, Faculty of Medicine, Prince of Songkla University, Hatyai, Songkhla, 90110, Thailand
[2] Department of Radiology, Faculty of Medicine, Prince of Songkla University, Hatyai, Songkhla, 90110, Thailand
[3] Department of Surgery, Faculty of Medicine, Prince of Songkla University, Hatyai, Songkhla, 90110, Thailand

(*Received December 12 2015, Accepted September 20 2016*)

Abstract. An advanced computational modeling has been playing an important role in medical applications. This study used a two-dimensional patient-specific model combined with computational fluid dynamics (CFD) to examine the relationship between the blood flow velocity ratio at the throat and the degrees of stenosis. The carotid artery geometries of three patients were determined and reconstructed from magnetic resonance angiography images. The assumption was that blood is an incompressible Newtonian fluid with steady and a rigid artery wall. Simulated degrees of stenosis were generated to make varied stenosis conditions. Blood flow velocity, pressure and wall shear stress in the study model were determined by CFD. The results showed that the blood flow velocity ratio at the throat significantly increased when the progress of stenosis increased from 30% to 70% on the common carotid artery. Wall shear stress ratio at the inner wall of the internal carotid artery decreased when the stenosis increased. Plotting the blood flow velocity ratio at the throat and the percentage of stenosis from these patient-specific models, the exponential function showed an appropriate relationship. Therefore, this exponential relationship can be advantageous for a pre-assessment of the degree of stenosis using the velocity obtained from a Doppler ultrasound measurement.

Keywords: patient-specific model, carotid stenosis, computational fluid dynamics, blood flow velocity, wall shear stress

1 Introduction

Carotid stenosis refers to abnormal narrowing of the carotid artery and is a leading cause of death and paralysis in patients with cardiovascular disease. Atherosclerosis, which is an accumulation of plaque at the vascular wall surface, is a primary cause of stenosis. High blood pressure or hypertension, smoking, hyperlipidemia, and diabetes mellitus are also notable risk factors of atherosclerosis[6, 13]. Patients are not diagnosed until they complain of weakness, by which time the disease is well progressed. It would be beneficial for these patients if the stenosis was detected and could be treated before it became severe. Various modern imaging techniques are available for cardiovascular diagnosis and assessment such as computer tomography (CT), Doppler ultrasound and magnetic resonance angiography (MRA). These techniques have benefits and limitations depending on the condition of the patient and their ability to pay. Doppler ultrasound is one of the tools

* We thank Dr. Ruedeekorn Suwannanon for helping with the Doppler ultrasound measurements and Dr. Nattapon Chantarapanich for suggestions about the computational fluid dynamics model analysis. We also thank the patients who participated in this study. The authors are appreciated Assoc. Prof. Pornchai Phukpattaranont for his advices on the manuscript preparation. We would like to thank Mr. David Patterson for English editing. This work was supported by a New Researcher Scholarship of the Ministry of Science and Technology, Scholarship Division and the National Science and Technology Development Agency-NSTDA (Grant♯ SCH-NR2012-181), and the Faculty of Medicine, Prince of Songkla University (Grant♯ 56-113-25-2-3).

† Corresponding author. *E-mail address*: surapong.c@psu.ac.th

available for noninvasive evaluation of carotid stenosis, with the advantage of no radiation risk but the disadvantage of having lower sensitivity than the MRA[5, 25]. For blood flow measurement, the Doppler ultrasound is cheaper and less time-consuming than the MRA and CT.

Presently, a computational modeling is an effective engineering tool which has been used to study many physiological systems, including the cardiovascular system. Computational fluid dynamics (CFD) modeling is a state of the art technique which plays an important role in investigating hemodynamics and blood flow behavior[1, 4, 17]. The geometry and measured parameters from patients becomes more interesting in patient-specific computational modeling. Using medical image information such as anatomical geometry from MRA or CT incorporated with CFD modeling can enhance the realistic results of computational work. Using CFD to study stenosis enables the researcher to demonstrate the actual hemodynamics at the throat and post-stenotic areas with various degrees of severity of carotid stenosis[2, 16]. Using this computational tool can provide more information on the degree of stenosis and provides deeper insight into various conditions involving carotid artery stenosis without the danger of inducing complications in real-life subjects. An important aspect of such modeling is to make possible the early detection of developing conditions, and thus allow early intervention to prevent serious problems to develop. Based on the combination of a real two-dimensional geometry of the carotid arteries in stenosis patients and CFD analysis, this study investigated a relationship between the degrees of carotid stenosis and the throat blood flow velocity ratio which is advantageous for carotid stenosis pre-assessment with Doppler ultrasound.

2 Methods

2.1 Anatomical geometry and blood flow velocity acquisition

Carotid artery geometries were obtained from three male patients through scanning with MRA using a 3.0T magnetic resonance imaging machine (Philip Achieva 3.0T x-Series MRI). Then, the patients were diagnosed by the doctor. Blood flow velocity in common the carotid artery was measured using a 7.5 MHz Doppler ultrasound (Toshiba, TUS-A500). We complied with the World Medical Association Declaration of Helsinki regarding ethical conduct of research involving human subjects. The study protocol was approved by the institutional review committee with the ethics number EC-56-113-25-2-3. The patients were recruited from a university hospital, and signed an informed consent form. We reconstructed the two-dimensional carotid geometry contour from MRA images using a computer-aided design (CAD) program. Also using CAD, various degrees of stenosis were generated in order to simulate progressive degrees of stenosis. The steps in the anatomical geometry reconstruction are demonstrated as a diagram in Fig. 1.

2.2 Computational models

Fifteen geometrical models used in this study were generated with the unstructured quadrilateral mesh by computational fluid dynamic analysis software. The quadrilateral mesh had an element length of 0.125 mm on a normal wall and 0.1 mm on a stenotic wall. Computational fluid dynamics was used to solve the continuity and momentum equations as shown in Eqs. (1) and (2). In our model, blood flow in the common carotid artery was assumed to be a turbulent flow and the artery wall to be a rigid body with no-slip conditions. Blood viscosity and blood density were assumed to be 1,050 kg·m^{-3} and 0.004 N·sec·m^{-2}, respectively. The velocity at the proximal common carotid artery obtained from Doppler ultrasound was assigned as an inflow velocity of the carotid artery and the pressure at the inlet and outlet of the boundary were equal to diastolic pressure for use in our computational fluid dynamic model analysis.

$$\nabla \cdot v = 0, \tag{1}$$

$$\rho\{(\partial v/\partial t) + v \cdot \nabla v\} = -\nabla p + \mu \nabla^2 v. \tag{2}$$

2.3 Data analysis

We calculated the blood velocity and blood pressure at the stenotic region and evaluated wall shear stress (WSS) at the wall surface of the internal carotid artery. At the stenotic area, blood velocity was converted into the blood velocity ratio by dividing the value of blood velocity by the value of the inlet velocity in the same patient as defined in Eq. (3).

$$\text{Blood flow velocity ratio} = \frac{V}{V_{\text{CCA}}}. \tag{3}$$

where V is the mean velocity at the location of interest and V_{CCA} is the inlet velocity in the common carotid artery obtained from the Doppler ultrasound.

The blood flow velocity ratio in each patient-specific model was examined against various percentage of stenosis. The relationship between the mean blood flow velocity ratio and the degree of stenosis was created based on data from three patients. The relationship was approximately fitted with either a linear or a nonlinear regression with 95% confidence interval (CI) to determine the best fitted result. In addition, a wall shear stress (WSS) ratio was calculated as expressed in Eq. (4).

$$\text{WSS ratio} = \frac{\text{WSS}}{\text{WSS}_{\text{CCA}}}. \tag{4}$$

where WSS is wall shear stress at the wall surface, either inner or outer, in the internal carotid artery and WSS_{CCA} is the maximum wall shear stress.

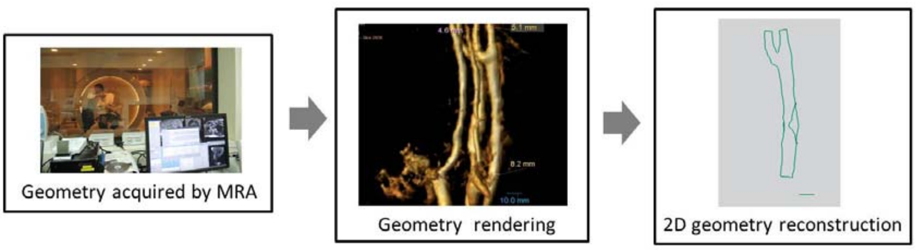

Fig. 1: Steps in the anatomical geometry reconstruction model used in the study

3 Results

Our study was based on the data from three male patients with a mean age of 61 years, all of whom had a history of high cholesterol, high blood pressure, and hyperglycemia. Their demographic data are presented in Tab. 1. The carotid artery geometry and various degrees of stenosis, both real and simulated, in each patient are demonstrated in Fig. 1. The stenosis was evident on both sides of the wall in patient ♯1 and ♯2 and only one side of the wall in patients ♯3. In addition, there were two stenotic regions at the common carotid artery in patient ♯2.

3.1 Carotid stenosis and blood flow velocity

The simulation results showed that the blood flow velocities at the stenotic region were higher than the inlet velocity in the patient-specific models as the velocity ratio was higher than 1. The blood flow velocity decreased immediately after passing the throat area and was lower than 1 near the bifurcation. Furthermore, the blood flow velocity in ICA was lower than the inlet velocity. Blood flow velocities also increased when the degree of stenosis increased (Fig. 3). However, in a multiple stenosis case as in patient ♯2 which had two areas of plaque accumulation, the blood flow velocity was more greatly decreased at the second stenotic region compared with the blood flow velocity at the first region.

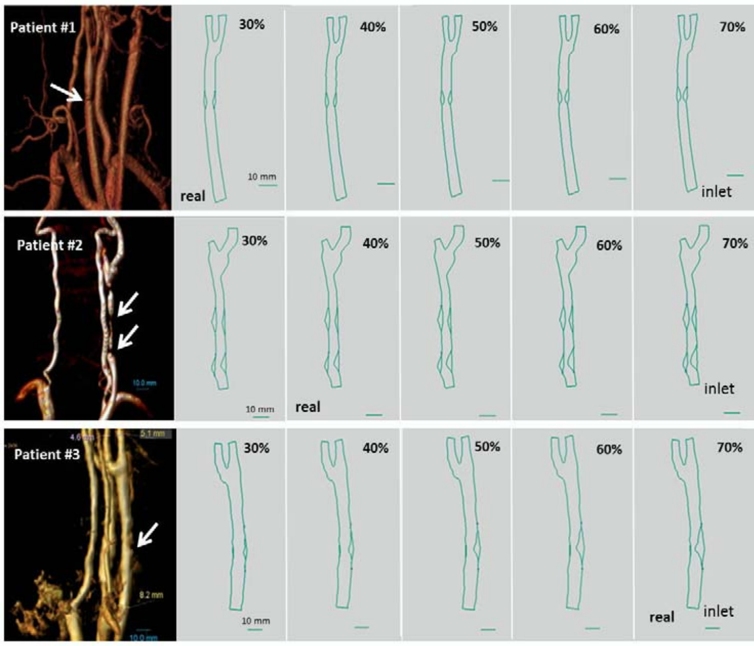

Fig. 2: Two dimensional patient-specific models of the carotid artery and various degrees of stenosis. White arrows indicate stenotic areas

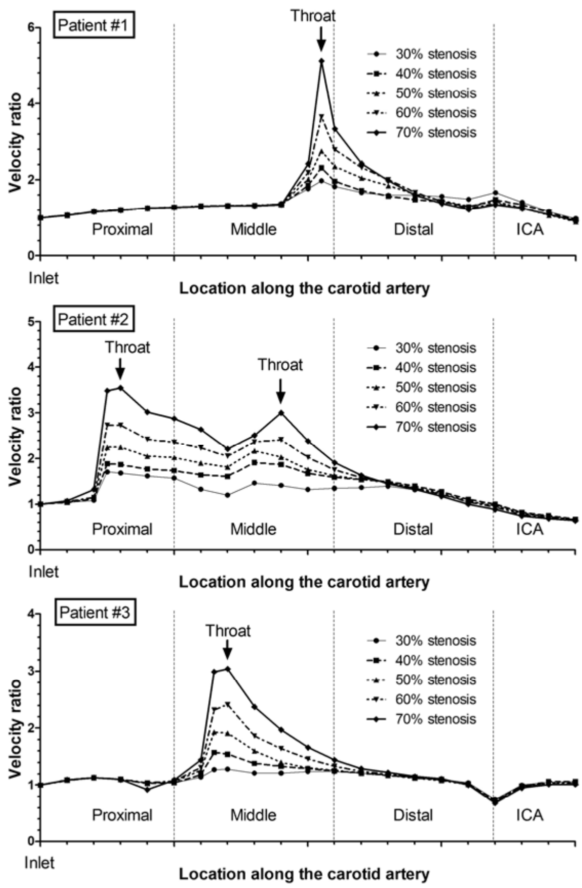

Fig. 3: Blood flow velocity ratio at each location along the carotid artery at the different degrees of stenosis

Table 1: Demographic data of patients

	Patients with carotid artery stenosis (n=3)
Gender	Male
Age (years)	61 ± 10
Height (m)	1.68 ± 0.11
Weight (kg)	70.00 ± 8.57
Body mass index (kg/m2)	24.64 ± 0.27
Systolic blood pressure (mmHg)	148 ± 13
Diastolic blood pressure (mmHg)	84 ± 18

3.2 Carotid stenosis and blood pressure

The blood pressure drop was clearly visible on the pressure color map as shown in Fig. 4. The maximum blood pressure located at the inlet of the common carotid artery. Reduced blood pressure at the throat was found. Moreover, blood pressure was higher at the bifurcation compared to the proximal area of bifurcation. All three patient models demonstrated similar results.

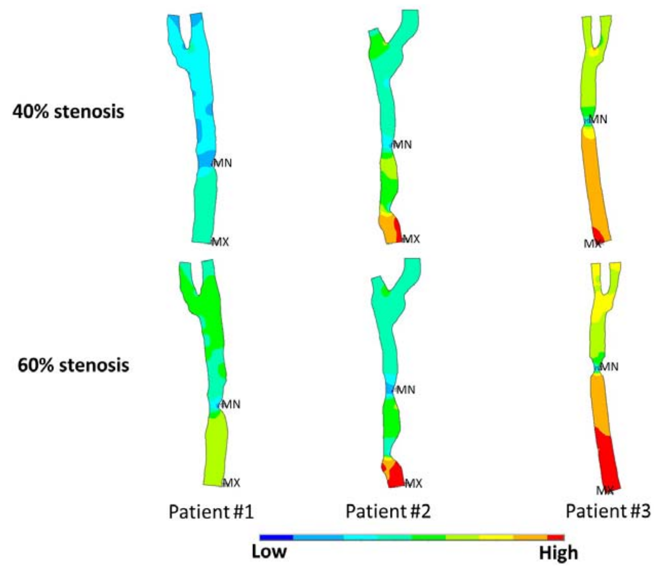

Fig. 4: Pressure color map in three patient-specific models at 40% and 60% stenosis. MX locates maximum pressure and MN locates minimum pressure

3.3 Carotid stenosis and wall shear stress

The maximum wall shear stresses at the stenotic region in each patient are shown in Table 2. The maximum wall shear stress increased when the degree of stenosis increased. Furthermore, the wall shear stress ratio at the inner wall of the ICA was higher than at the outer wall, as demonstrated in Fig. 5. The wall shear stress ratios at both the inner and outer walls of the ICA decreased as the stenosis progressed.

3.4 Relationship between the blood flow velocity ratio and the degree of stenosis

The means of blood flow velocity ratio at the throat of all three patient-specific models were plotted against the degrees of stenosis as shown in Fig. 6. A linear regression with a 95% confidence interval (CI) and two nonlinear regressions, exponential and second-order polynomial equations, with 95% CI, were applied to fit the data. The equation and coefficient of determination (r^2) of each fitted relationship are demonstrated in Fig. 6. The exponential relationship was a preferable fit with an acceptable 95% CI, a narrower range, compared with other fits, especially when the degree of stenosis was less than 20%.

Table 2: Maximum wall shear stress in each patient with various degrees of stenosis

Degree of stenosis	Maximum wall shear stress (N/m^2)		
	Patient ♯1	Patient ♯2	Patient ♯3
30%	0.021	0.016	0.059
40%	0.024	0.017	0.081
50%	0.038	0.021	0.121
60%	0.043	0.026	0.140
70%	0.054	0.037	0.196

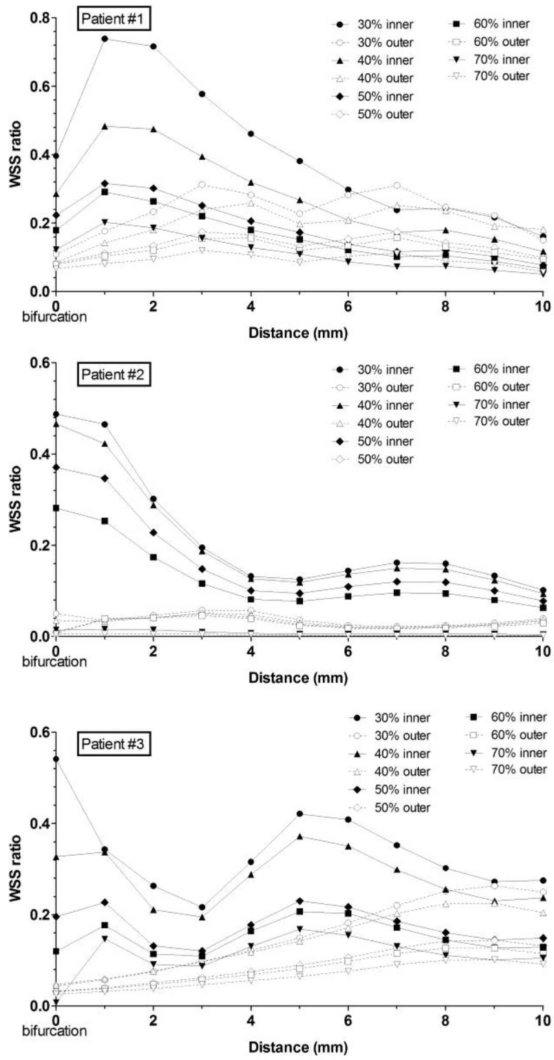

Fig. 5: Wall shear stress ratios at the inner wall and outer wall of the internal carotid artery (ICA) at the different degrees of stenosis

4 Discussion

Patient-specific models for the carotid artery stenosis using MRA-acquired geometry and computational fluid dynamics were constructed in this study to look at the hemodynamic changes. An exponential relationship between the velocity ratio at the throat and the degree of stenosis was a suitable fit function with an acceptable 95% CI. This relationship can help the physician to predetermine the degree of stenosis in the common carotid artery in patients at risk of this complication. Our computational results using the vascular geometry obtained from real patients showed that vascular stenosis increased blood flow velocity and reduced blood pressure across the stenotic region. In this situation, the increase in blood flow velocity and the decrease in blood pressure at the throat is due to the reduction of flow area, in a way similar to the flow passing through

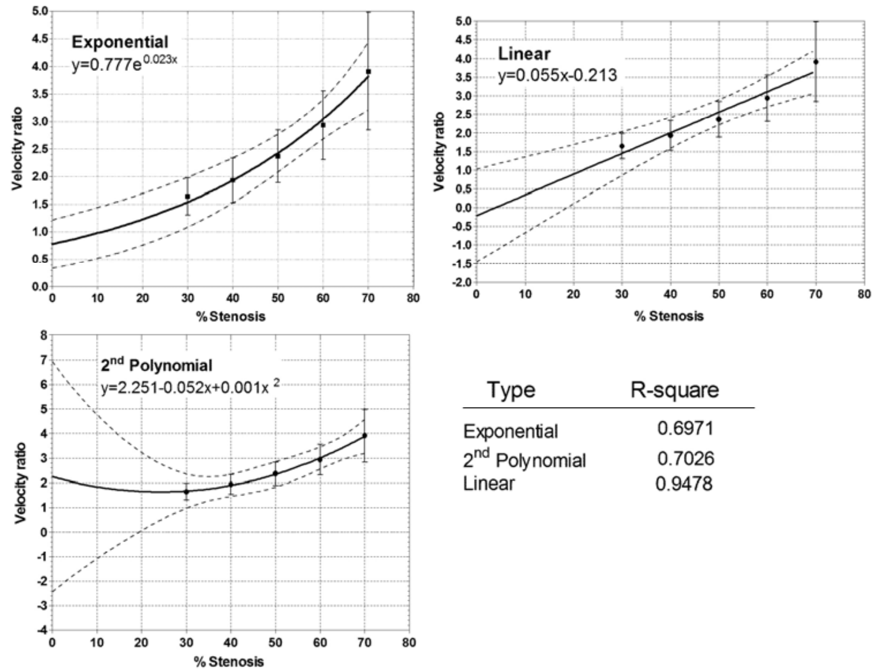

Type	R-square
Exponential	0.6971
2nd Polynomial	0.7026
Linear	0.9478

Fig. 6: Linear and nonlinear relationships with 95% confidence intervals between the blood flow velocity ratio at the throat and the degrees of stenosis. R-square is the square of the correlation coefficient

a jet nozzle[10, 18, 24]. After passing the throat, the blood flow velocity rapidly drops, which is similar to flowing through the expander[10]. These behaviors can be explained by the Bernoulli's principle.

Most studies focused on carotid artery stenosis have reported that hemodynamic factors critically change at the stenotic region located at either the common carotid artery or the internal carotid artery[11, 14]. One study demonstrated that the maximum and mean velocities in the carotid artery apparently increased when the stenosis degree changed from mild to moderate and then to severe[23]. But their study reported that there was no significant difference in velocity between the stenosis degrees. Simulation results from another study using a patient-specific model with a high degree of stenosis showed that the maximum velocity occurred at the throat and the velocity streamline became a swirling flow after the throat[24]. Similarly, our results in three patient-specific models demonstrated that maximum blood flow velocity occurred at the stenotic region, higher by 3-5 times than the inlet velocity. Furthermore, our study found that multiple stenotic regions profoundly affected the blood flow velocity at the downstream side. Therefore, the flow behavior is affected by the number and location of stenotic areas as well as the vascular geometry.

Wall shear stress is an important parameter which is related to plaque initiation and progression in the carotid artery. Wall shear stress is high along the inner wall of the internal carotid artery while low wall shear stress is found in the external carotid artery[23]. A study in atherosclerotic plaque erosion in rabbits by Sameshima et al. reported that the site of erosive injury tended to occur at areas of high shear stress[19]. Low wall shear stress has been shown to be associated with atherosclerosis[9, 12, 21]. Our study found that wall shear stress at the throat increased with the degree of stenosis, which was also found in the studies of Li et al. and Caiazzo et al.[3, 24]. In our study, the stenotic regions located at the common carotid artery and the internal carotid artery was downstream of the sites of stenosis. We found that the wall shear stress along the inner wall of the internal carotid artery was higher than at the outer wall of the internal carotid artery. Furthermore, the wall shear stress at the inner wall of the internal carotid artery decreased when the degree of stenosis increased. This finding is similar to the findings of a study by Caiazzo and colleagues, which reported that wall shear stress decreased when the reduction of diameter at the stenotic region increased[3]. That means the location of stenosis influences wall shear stress, which might introduce the onset of atherosclerosis around the area of low wall shear stress.

Several studies have proposed the use of velocity related parameters to assess or evaluate carotid artery stenosis. These parameters are such as the ratio between the internal carotid systolic velocity (ICSV) at the carotid bulb and the distal internal carotid systolic velocity (DICSV) and diastolic velocity ratios[8, 22]. For example, Soulez et al. showed that the ICSV/DICSV ratio was useful when attempting Doppler detection of carotid artery stenosis if the ICSV was greater than 100 cm/s[22]. In addition, Lee and colleagues found that the variability of common carotid artery (CCA) velocities can affect interpretation of ICA/CCA ratios and the end-diastolic velocity threshold provided higher sensitivity for the detection of ICA stenosis than the peak systolic velocity threshold[15]. These ideas have been proposed as useful in assessing the risk level of stroke using Doppler ultrasound. However, some studies have shown that maximum peak systolic velocity in the ICA is more accurate than the velocity ratio[7, 20]. From another viewpoint, our results suggest that the relationship between the ratio of throat velocity and inlet velocity in CCA (V_T/V_{CCA}) and degree of stenosis was properly fitted by an exponential function with a good coefficient of determination (r^2) and the better range of 95% CI. Regarding to the advantages of Doppler ultrasound, low cost service and non-complicate operation, compared to MRA or CT, this relationship might be advantageous for physicians to practically use to prescreen patients by referring the blood velocity measured by Doppler ultrasound to this relationship chart.

There were several limitations in the current study. One of them was that only three patients were acquired for the carotid artery geometry and inlet velocity to use in our computation. Thus, based on this number of patients, the exponential relationship might provide only the tendency of the degree of stenosis. Moreover, several assumptions were set for the CFD simulation, such as rigid vessel wall, steady flow and no plaque material conditions, which could be different than actual in situ conditions. The 2D carotid geometry and some MRA image artifacts in our study are also another limitation that could cause our results to be different from real situation. Therefore, it is necessary to overcome these limitations in future studies to obtain more realistic hemodynamic parameters and a good pre-assessment for stenosis.

5 Conclusions

Computational fluid dynamics with a patient-specific model demonstrated that stenosis in the common carotid artery increased blood velocity and wall shear stress but lowered blood pressure at the throat. The flow behavior is affected by the number and location of stenotic areas as well as the vascular geometry. The exponential relationship between the velocity ratio at the throat and the degree of stenosis might be useful for a pre-assessment of stenosis degree using Doppler ultrasound measurement. However, several limitations in this study need to be resolved for better simulation results.

References

[1] B. B. Ariff. Carotid artery hemodynamics: observing patient-specific changes with amlodipine and lisinopril by using mr imaging computation fluid dynamics. *Radiology*, 2010, **257**(3): 662–9.

[2] R. Balossino, G. Pennati, F. Migliavacca, L. Formaggia, A. Veneziani, M. Tuveri, G. Dubini. Computational models to predict stenosis growth in carotid arteries: which is the role of boundary conditions? *Computer Methods in Biomechanics & Biomedical Engineering*, 2009, **12**(1): 113–23.

[3] A. Caiazzo, G. Montecinos, L. O. Mller, E. M. Haacke, E. F. Toro. Computational haemodynamics in stenotic internal jugular veins. *Journal of Mathematical Biology*, 2015, **70**(4): 745–772.

[4] T. Chaichana, Z. Sun, J. Jewkes. Hemodynamic impacts of left coronary stenosis: a patient-specific analysis. *Acta of Bioengineering & Biomechanics*, 2013, **15**(3): 107–12.

[5] A. C. Chao, C. M. Chern, T. B. Kuo, C. H. Chou, Y. M. Chuang, W. J. Wong, H. H. Hu. Noninvasive assessment of spontaneous baroreflex sensitivity and heart rate variability in patients with carotid stenosis. *Cerebrovascular Diseases*, 2003, **16**(2): 151–7.

[6] P. A. Dharmasaroja, K. Intharakham. Risk factors for carotid stenosis in thai patients with ischemic stroke/tia. *Angiology: The Journal of Vascular Diseases*, 2010, **61**(8): 789–92.

[7] W. E. Faught, M. A. Mattos, P. S. van Bemmelen, K. J. Hodgson, L. D. Barkmeier, D. E. Ramsey, D. S. Sumner. Color-flow duplex scanning of carotid arteries: new velocity criteria based on receiver operator characteristic analysis for threshold stenoses used in the symptomatic and asymptomatic carotid trials. *Journal of Vascular Surgery*, 1994, **19**(5): 818–828.

[8] S. G. Friedman, B. Hainline, A. W. Feinberg, M. L. Lesser, B. A. Napolitano. Use of diastolic velocity ratios to predict significant carotid artery stenosis. *Stroke*, 1988, **19**(7): 910–2.

[9] A. Gnasso, C. Irace, C. Carallo, M. S. De Franceschi, C. Motti, P. L. Mattioli, A. Pujia. In vivo association between low wall shear stress and plaque in subjects with asymmetrical carotid atherosclerosis. *Stroke; a journal of cerebral circulation*, 1997, **28**(5): 993–8.

[10] P. Hariharan, M. Giarra, V. Reddy, S. W. Day, K. B. Manning, S. Deutsch, S. F. Stewart, M. R. Myers, M. R. Berman, G. W. Burgreen. Multilaboratory particle image velocimetry analysis of the fda benchmark nozzle model to support validation of computational fluid dynamics simulations. *Journal of Biomechanical Engineering*, 2011, **133**(4): 219–231.

[11] R. D. Henderson, D. A. Steinman, M. Eliasziw, H. J. Barnett. Effect of contralateral carotid artery stenosis on carotid ultrasound velocity measurements. *Stroke; a journal of cerebral circulation*, 2000, **31**(11): 2636–40.

[12] Y. Jiang, K. Kohara, K. Hiwada. Low wall shear stress contributes to atherosclerosis of the carotid artery in hypertensive patients. *Hypertension Research Official Journal of the Japanese Society of Hypertension*, 1999, **22**(3): 203–7.

[13] C. H. Jung, B. Y. Kim, K. J. Kim, S. H. Jung, C. H. Kim, S. K. Kang, J. O. Mok. Contribution of subcutaneous abdominal fat on ultrasonography to carotid atherosclerosis in patients with type 2 diabetes mellitus. *Cardiovascular Diabetology*, 2014, **13**(1): 1–8.

[14] S. M. A. Khader, B. S. Shenoy, R. Pai, S. G. Kamath, N. M. Sharif, V. R. K. Rao. Effect of increased severity in patient specific stenosis of common carotid artery using cfdła case study. *World Journal of Modelling & Simulation*, 2011, **7**(2): 113–122.

[15] V. S. Lee, B. S. Hertzberg, M. J. Workman, T. P. Smith, M. A. Kliewer, D. M. Delong, B. A. Carroll. Variability of doppler us measurements along the common carotid artery: effects on estimates of internal carotid arterial stenosis in patients with angiographically proved disease. *Radiology*, 2000, **214**(2): 387–92.

[16] I. Marshall, S. Zhao, P. Papathanasopoulou, P. Hoskins, Y. Xu. Mri and cfd studies of pulsatile flow in healthy and stenosed carotid bifurcation models. *Journal of Biomechanics*, 2004, **37**(5): 679–687.

[17] D. Martin, A. Zaman, J. Hacker, D. Mendelow, D. Birchall. Analysis of haemodynamic factors involved in carotid atherosclerosis using computational fluid dynamics. *British Journal of Radiology*, 2009, **82 Spec No 1**(special issue 1): S33–S38.

[18] I. Olaru. The fluid flow simulation through to a venturi nozzle. *Journal of Engineering Studies & Research*, 2013, **19**(2).

[19] N. Sameshima, A. Yamashita, S. Sato, S. Matsuda, Y. Matsuura, Y. Asada. The values of wall shear stress, turbulence kinetic energy and blood pressure gradient are associated with atherosclerotic plaque erosion in rabbits. *Journal of Atherosclerosis & Thrombosis*, 2014, **21**(8): 831–838.

[20] S. W. Schwartz, L. E. Chambless, W. H. Baker, J. P. Broderick, G. Howard. Consistency of doppler parameters in predicting arteriographically confirmed carotid stenosis. asymptomatic carotid atherosclerosis study investigators. *Stroke*, 1997, **28**(2): 343–7.

[21] P. Siogkas, A. Sakellarios, T. P. Exarchos, L. Athanasiou, E. Karvounis, K. Stefanou, E. Fotiou, D. I. Fotiadis, K. K. Naka, L. K. Michalis. Multiscale-patient-specific artery and atherogenesis models. *IEEE transactions on bio-medical engineering*, 2011, **58**(12): 3464–8.

[22] G. Soulez, E. Therasse, P. Robillard, A. Fontaine, N. Denbow, P. Bourgouin, V. L. Oliva. The value of internal carotid systolic velocity ratio for assessing carotid artery stenosis with doppler sonography. *American Journal of Roentgenology*, 1999, **172**(1): 207–12.

[23] B. Sui, P. Gao, Y. Lin, L. Jing, S. Sun, H. Qin. Hemodynamic parameters distribution of upstream, stenosis center, and downstream sides of plaques in carotid artery with different stenosis: a mri and cfd study. *Acta Radiologica*, 2015, **56**(3): 347–54.

[24] F. P. P. Tan. Flow pattern analysis in a highly stenotic patient-specific carotid bifurcation model using a turbulence model. *Computer Methods in Biomechanics & Biomedical Engineering*, 2014, **18**(10): 1099–1107.

[25] J. M. Wardlaw, F. M. Chappell, J. J. Best, K. Wartolowska, E. Berry. Non-invasive imaging compared with intra-arterial angiography in the diagnosis of symptomatic carotid stenosis: a meta-analysis. *International Journal of Emergency & Critical Care Medicine*, 2006, **367**(9521): 1503–12.